

Publisher: GSA
Journal: GEOL: Geology
DOI:10.1130/G38051.1

1 Rolling open Earth's deepest forearc basin

2 **Jonathan M. Pownall¹, Robert Hall², and Gordon S. Lister¹**

3 *¹Research School of Earth Sciences, Australian National University, Canberra, ACT*
4 *2601, Australia*

5 *²SE Asia Research Group, Department of Earth Sciences, Royal Holloway University of*
6 *London, Egham TW20 0EX, UK*

7 **ABSTRACT**

8 The Weber Deep—a 7.2 km-deep forearc basin within the tightly curved Banda
9 Arc of eastern Indonesia—is the deepest point of the Earth's oceans not within a trench.
10 Several models have been proposed to explain the tectonic evolution of the Banda Arc in
11 the context of the ongoing (*c.* 23 Ma–present) Australia–SE Asia collision, but no model
12 explicitly accounts for how the Weber Deep achieved its anomalous depth. Here we
13 propose the Weber Deep formed by forearc extension driven by eastward subduction
14 rollback. Substantial lithospheric extension in the upper plate was accommodated by a
15 major, previously unidentified, low-angle normal fault system we name the 'Banda
16 Detachment'. High-resolution bathymetry data reveal that the Banda Detachment is
17 exposed underwater over much of its 120 km down-dip and 450 km lateral extent, having
18 produced the largest bathymetric expression of any fault discernable in the world's
19 oceans. The Banda Arc is a modern analogue for highly extended terranes preserved in
20 the many regions that may similarly have 'rolled open' behind migrating subduction
21 zones.

22 **INTRODUCTION**

23 A subducting slab will sweep backward through the mantle if its negative
24 buoyancy overcomes the mantle's viscous drag. This action—slab rollback—will drive a
25 trench to migrate in the opposite direction to that of subduction, thereby enabling an arc
26 to travel considerable distances and continually adjust its curvature (Dewey, 1980;
27 Royden, 1993). Rollback may cause an adjacent mountain belt to switch between periods
28 of shortening and extension (Lister and Forster, 2009), drive the extension of back-arc
29 and forearc basins (e.g., D'Agostino et al., 2011; Maffione et al., 2015; Do Couto et al.,
30 2016), exhume metamorphic core complexes (e.g., Lister et al., 1984; Dewey, 1988),
31 and/or cause oroclinal bending (e.g., Schellart and Lister, 2004). These first-order
32 tectonic processes are intrinsic to the evolution of many, if not all, mountain belts;
33 however, they are typically very difficult to identify once active deformation ceases.
34 Consequently, the influence of slab rollback on the formation of mature and ancient
35 mountain belts and basins is poorly understood. Here we demonstrate how slab rollback
36 was fundamental to basin formation within the tightly-curved Banda Arc of eastern
37 Indonesia (Fig. 1) – importantly one of very few places where active subduction can be
38 related to geological observations of modern orogenesis.

39 **TECTONIC CONTEXT**

40 The Banda Arc (Fig. 1, 2), due to its extreme 180° curvature, is often cited as a
41 'classic' example of a modern orocline (e.g., Schellart and Lister, 2004). Jurassic oceanic
42 lithosphere was subducted at the trench, beneath the Neogene Banda Sea, to form a
43 highly concave westward-plunging synform that at present reaches the 660 km-depth
44 mantle discontinuity (Spakman and Hall, 2010; Hall and Spakman, 2015). Although
45 some authors have argued that this highly concave slab geometry was created by two

46 independent subduction zones with opposite polarities (e.g., Cardwell and Isacks, 1978),
47 there is now considerable evidence that it once comprised a single slab, deformed during
48 slab rollback (e.g., Hamilton, 1979; Hall and Wilson, 2000; Milsom, 2001; Spakman and
49 Hall, 2010; Hall, 2011, 2012; Pownall et al., 2013).

50 Unlike most modern arcs, the Banda Arc does not preserve an oceanic trench
51 since the rolling-back subduction zone has collided with the Australian continental
52 margin. It has been proposed that the shape of this margin from the Jurassic
53 approximated the modern Banda Arc (Hall, 2011), enclosing a D-shaped ‘Banda
54 Embayment’ of dense Jurassic oceanic crust (the Proto-Banda Sea), that was readily
55 subducted on arrival at the eastward-migrating trench (Spakman and Hall, 2010). Upon
56 arc–continent collision, some buoyant continental crust of the Banda Embayment margin
57 may have entered the upper mantle in the final stages of subduction (Royden and Husson,
58 2009; Tate et al., 2015). During this time, there was thrusting towards the Australian
59 continental margin to form the Seram Trough, the Timor Trough, and their adjacent fold-
60 and-thrust belts.

61 Banda slab rollback has driven upper-plate extension since c. 16 Ma (Pownall et
62 al., 2014), opening the North Banda Basin (Fig. 2) between 12.5 and 7.2 Ma, and the
63 South Banda Basin between 6.5 and 3.5 Ma (Hinschberger et al., 2005). However, it
64 remains unclear what caused the lithosphere beneath the easternmost Banda Sea to
65 subside to its present depth of 7.2 km. Some authors have suggested it formed as a
66 flexural response to a tightening of the Banda Arc’s curvature (Bowin et al., 1980) or the
67 thrusting of the Banda Sea over the surrounding buoyant Australian continental margin
68 (Hamilton, 1979). Others, who instead interpreted the Weber Deep as an extensional

69 basin (Charlton et al., 1991; Hinschberger et al., 2005; Spakman and Hall, 2010; Hall,
70 2011, 2012), attributed E–W extension either directly to N–S shortening driven by the
71 northward advance of Australia (Charlton et al., 1991), or to eastward slab rollback
72 (Spakman and Hall, 2010; Hall, 2011, 2012) as discussed previously. The Weber Deep
73 has also been explained as simply the result of sinking of the underlying Banda slab
74 (Bowin et al., 1980; McCaffrey, 1988) without the requirement of rollback.

75 Here, we propose that basin extension and subsidence were driven by the final
76 stages of Banda Slab rollback, and accommodated by extension along a vast but
77 previously-undocumented low-angle normal fault system—the Banda Detachment—
78 whose scarps form the eastern wall and floor of the Weber Deep.

79 **EVIDENCE FOR THE BANDA DETACHMENT**

80 **Bathymetric Analysis**

81 Figures 1 and 3 are images derived from 15 m resolution MULTIBEAM
82 bathymetry data of the eastern Banda Arc, which cover the Weber Deep and the Aru
83 Trough. Significantly, these data show corrugated landforms on inliers within the abyssal
84 sedimentary infill. The ridges and grooves of these features are straight, and are sub-
85 parallel (within 10°) with consistent NW–SE orientations across the entire basin floor
86 (Fig. 1). The grooves are most pronounced in the northern (Fig. 3A), western (Fig. DR1
87 in the GSA Data Repository¹), and southern (Fig. 3B, DR2) parts of the Weber Deep,
88 below 3 km depth. Large submarine slumps have blanketed much of the eastern rise.

89 We interpret these lineated surfaces to comprise the footwall of a low-angle
90 normal fault system (following Spencer, 2010) that closely approximates the morphology
91 of the entire floor and outer wall of the easternmost Banda Sea. The grooved surfaces

92 could belong to a single low-angle fault, although they could alternatively mark
93 subsidiary normal faults that shallow into a master detachment at slightly greater depth.
94 The 'Banda Detachment' has a listric geometry, curving from a 12° dip adjacent to the
95 eastern rim of the basin, to horizontal beneath the abyssal sedimentary infill, and
96 becoming slightly back-rotated (by 1°) adjacent to the volcanic arc. We also interpret the
97 grooves' orientation and collective length to record a southeasterly slip direction of 120–
98 130°, along which the 450 km-long detachment must have slipped > 120 km. To our
99 knowledge, this is the largest normal fault system exposed anywhere in the world's
100 oceans.

101 **Geological Evidence**

102 Seram and Ambon (Fig. 1) have undergone considerable lithospheric extension
103 throughout much of the Neogene (Pownall et al., 2013, 2014), attributed to their eastward
104 movement above the rolling-back Banda Slab (Spakman and Hall, 2010; Hall, 2011,
105 2012). Initially, this extension exhumed hot, predominantly lherzolitic mantle rocks to
106 shallow depths (~30 km), inducing melting and granulite-facies metamorphism of
107 adjacent crust under ultrahigh-temperature (UHT; > 900 °C) conditions (Pownall et al.,
108 2014; Pownall, 2015). Since *c.* 6.5 Ma, peridotites and high-temperature migmatites of
109 the resulting Kobipoto Complex (Pownall, 2015) have been exhumed beneath low-angle
110 detachment faults to the present-day exposure level across Seram (Pownall et al., 2013).

111 Our new field observations in the Wai Leklekan Mountains of eastern Seram
112 (130.46°E, 3.62°S), and on the small Banda Arc islands of Tioor, Kasiui, Kur, and Fadol
113 SE, of Seram (see Fig. 1), corroborate reports by Hamilton (1979), Bowin et al. (1980),
114 Charlton et al. (1991) and Honthaas et al. (1997) of ultramafic rock and migmatite

115 outcrops. In addition, we identified low-angle (12°) fault scarps in southeast Seram (Fig.
116 4A) and on Fadol (Fig. 4B) that we interpret as surface expressions of the Banda
117 Detachment (Fig. 1). Low-angle extensional shear zones were also observed on the south
118 coast of Kasiui (Fig. DR3). On Fadol, where ultramafic rocks and felsic gneisses
119 comprise the footwall (Fig. 4B), a normal shear sense fault is the only way to account for
120 the exhumation of upper-mantle/lower-crustal rocks (plus overlying Quaternary reefs)
121 immediately adjacent to the 7 km Weber Deep.

122 We therefore propose that peridotites exposed around the eastern Banda Arc, like
123 the ultramafic rocks in western Seram, must have been exhumed from the shallow
124 mantle, and are not fragments of ophiolites. The similarity in ages of gneisses on Seram
125 (*c.* 16 Ma U–Pb zircon and $^{40}\text{Ar}/^{39}\text{Ar}$ biotite ages; Pownall et al., 2013) and on Kur (*c.* 17
126 Ma K–Ar ages; Honthaas et al., 1997) further support a similar origin for exhumed lower
127 crustal/upper mantle complexes around the northern and eastern Banda Arc.

128 A final piece of evidence is that the grooves on the fault surfaces of the Weber
129 Deep run parallel to strike-slip faults within the Kawa Shear Zone (KSZ) on Seram (Fig.
130 1) – a major lithospheric fault zone incorporating slivers of exhumed mantle (Pownall et
131 al., 2013). The Banda Detachment converges with the KSZ, and we interpret them as part
132 of the same system. We infer the KSZ must have functioned as a right-lateral continental
133 transform east of 129.5°E in order to have separated NW–SE extension on the Banda
134 Detachment from contraction on land in northern Seram and offshore. Although the
135 current geomorphological expression of the KSZ indicates a left-lateral shear sense, there
136 is microstructural evidence for a complex history of both left- and right-lateral motions
137 (Pownall et al., 2013).

138 **“ROLLING OPEN” THE WEBER DEEP**

139 To account for extension of the Weber Deep in a 130–310° direction, we interpret
140 the driving force—rollback of the Banda Slab—to have followed the same southeastward
141 trajectory. This inference is consistent with previous reconstructions by Spakman and
142 Hall (2010) and Hall (2011, 2012), which depict southeastward migration of the Banda
143 subduction zone over the last 10 myr. These plate reconstructions further suggest that the
144 Weber Deep began to extend at 2 Ma (Hall, 2011, 2012), or alternatively 3 Ma
145 (Hinschberger et al., 2005), during the final stages of rollback, synchronous with arc–
146 continent collision. The relatively thin cover of basin-floor sediments (Hamilton, 1979;
147 Bowin et al., 1980) is indicative of young and rapid subsidence of the Weber Deep. The
148 depth of the basin may also have been enhanced by downward flexure of the underlying
149 (gently-dipping) Australian continental margin in response to the downward pull of the
150 connected oceanic slab, as suggested for the shallower Western Alboran Basin which
151 formed in a similar rollback setting in the Betic-Rif Arc (Do Couto et al., 2016).

152 As illustrated in Figure 5, the Banda Detachment must bound the upper surface of
153 a lithospheric wedge, likely derived from the fragmented Sula Spur (Bowin et al., 1980;
154 Hall, 2011, 2012), that was transported southeast and thrust over the Banda Embayment
155 continental margin. There is a terrane stack (cf. Lister and Forster, 2009, 2016) of
156 Australian crust and lithospheric mantle slices, sandwiched between the Banda
157 Detachment and the Frontal Thrust (labeled in Fig. 5). As observed, this stack includes
158 lherzolites and high-temperature migmatites of the Kobipoto Complex (Pownall, 2015),
159 and a number of core complexes which crop out across Seram, Ambon, and around the
160 eastern archipelago.

161 There is no evidence from recent seismicity that the Banda Detachment is
162 currently active. However, slip along the low-angle fault could feasibly operate through
163 aseismic creep (e.g., Hreinsdóttir and Bennett, 2009), or may occur infrequently during
164 catastrophic large-magnitude earthquakes (Wernicke, 1995). If the detachment is no
165 longer active, its prominent topographic expression (Fig. 4) would suggest that its
166 operation has only recently ceased.

167 **CONCLUSIONS AND WIDER IMPLICATIONS**

168 We conclude that southeastward rollback of the Banda slab since *c.* 2 Ma (Hall,
169 2011, 2012) drove substantial extension of its forearc, accommodated principally by the
170 450 km-long Banda Detachment, to form the 7.2 km Weber Deep (Fig. 5). Before this
171 (16–2 Ma), the rolling-back Banda Slab was forced by the resistance of the D-shaped
172 Australian continental margin to adopt its extreme curvature, which in turn drove the
173 lithospheric extension, mantle exhumation, crustal melting, and high-temperature
174 metamorphism across the northern and eastern arc. The Banda Arc illustrates how slab
175 rollback in the modern Earth may drive oroclinal bending and substantial extension of
176 outer arc and forearc regions.

177 The Banda Detachment and Weber Deep may be amongst the largest of their kind
178 in the modern Earth, but they are similar in scale to many ‘fossil’ examples preserved in
179 older terranes. For instance, the Banda Detachment’s listric geometry, ‘upwarping’
180 toward the volcanic arc (cf. Spencer, 1984), and size, are all analogous to detachment
181 faults characterizing the western USA’s Basin-and-Range Province (e.g., Lister and
182 Davis, 1989). Furthermore, the grooved fault surfaces in the Weber Deep are similar in
183 morphology and scale to the ‘turtlebacks’ (Wright et al., 1974) of California and Nevada.

184 It is a distinct possibility that several older highly-extended terranes, such as the Basin-
185 and-Range, may have also formed in response to major rollback events (cf. Dewey, 1980,
186 1988; Lister et al., 1984; Royden, 1993) for which eastern Indonesia is a rare modern
187 analogue.

188 **ACKNOWLEDGMENTS**

189 The authors are grateful to TGS and GeoData Ventures Pte. Ltd. for use of their
190 high-resolution multibeam bathymetry data set. We thank A. Trihatmojo and I.M.
191 Watkinson for field assistance, L. Jolivet, D.J.J. van Hinsbergen, and M. Sandiford for
192 constructive reviews, and editor R. Holdsworth. This work was funded by the SE Asia
193 Research Group (Royal Holloway University of London) and Australian Research
194 Council grants DE160100128 (awarded to JMP), and DP120103554 and LP130100134
195 (awarded to GSL).

196 **REFERENCES CITED**

197 Bowin, C., Purdy, G.M., Johnston, C., Shor, G., Lawver, L., Hartono, H.M.S., and Jezek,
198 P., 1980, Arc-Continent Collision in Banda Sea Region: AAPG Bulletin, v. 64,
199 p. 868–915.

200 Cardwell, R.K., and Isacks, B.L., 1978, Geometry of the subducted lithosphere beneath
201 the Banda Sea in Eastern Indonesia from seismicity and fault plane solutions: Journal
202 of Geophysical Research, v. 83, p. 2825–2838, doi:10.1029/JB083iB06p02825.

203 Charlton, T.R., Kaye, S.J., Samodra, H., and Sardjono, 1991, Geology of the Kai Islands:
204 Implications for the evolution of the Aru Trough and Weber Basin, Banda Arc,
205 Indonesia: Marine and Petroleum Geology, v. 8, p. 62–69, doi:10.1016/0264-
206 8172(91)90045-3.

- 207 Dewey, J.F., 1980, Episodicity, sequence, and style at convergent plate boundaries, *in*
208 Strangway, D.W., ed., The continental crust and its mineral deposits: Geological
209 Association of Canada Special Paper 20, p. 553–573.
- 210 Dewey, J.F., 1988, Extensional collapse of orogens: *Tectonics*, v. 7, p. 1123–1139,
211 doi:10.1029/TC007i006p01123.
- 212 D’Agostino, N., D’Anastasio, E., Gervasi, A., Guerra, I., Nedimović, M.R., Seeber, L.,
213 and Steckler, M., 2011, Forearc extension and slow rollback of the Calabrian Arc
214 from GPS measurements: *Geophysical Research Letters*, v. 38, L17304,
215 doi:10.1029/2011GL048270.
- 216 Do Couto, D., Gorini, C., Jolivet, L., Lebret, N., Augier, R., Gumiaux, C., d’Acremont,
217 E., Ammar, A., Jabour, H., and Auxietre, J.-L., 2016, Tectonic and stratigraphic
218 evolution of the Western Alboran Sea Basin in the last 25 Myrs: *Tectonophysics*, v.
219 677–678, p. 280–311, doi:10.1016/j.tecto.2016.03.020.
- 220 Hall, R., 2011, Australia–SE Asia collision: plate tectonics and crustal flow, *in* Hall, R.,
221 Cottam, M.A., and Wilson, M.E.J., eds., *The SE Asian Gateway: History and*
222 *Tectonics of the Australia–Asia Collision*: London, Geological Society [London]
223 Special Publication 355, p. 75–109, doi:10.1144/SP355.5.
- 224 Hall, R., 2012. Late Jurassic–Cenozoic reconstructions of the Indonesian region and the
225 Indian Ocean: *Tectonophysics* v. 570, p. 1–41, doi:10.1016/j.tecto.2015.07.003.
- 226 Hall, R., and Wilson, M.E.J., 2000, Neogene sutures in eastern Indonesia: *Journal of*
227 *Asian Earth Sciences*, v. 18, p. 781–808, doi:10.1016/S1367-9120(00)00040-7.
- 228 Hall, R., and Spakman, W., 2015, Mantle structure and tectonic history of SE Asia:
229 *Tectonophysics*, v. 658, p. 14–45, doi:10.1016/j.tecto.2015.07.003.

- 230 Hamilton, W., 1979, Tectonics of the Indonesian Region: USGS Professional Paper, v.
231 1078, 345 p.
- 232 Hinschberger, F., Malod, J.-A., Réhault, J.-P., Villeneuve, M., Royer, J.-Y., and
233 Burhanuddin, S., 2005, Late Cenozoic geodynamic evolution of eastern Indonesia:
234 Tectonophysics, v. 404, p. 91–118, doi:10.1016/j.tecto.2005.05.005.
- 235 Honthaas, C., Villeneuve, M., Réhault, J.-P., Bellon, H., Cornée, J.-J., Saint-Marc, P.,
236 Butterlin, J., Gravelle, M., and Burhanuddin, S., 1997, L'île de Kur: Géologie du
237 flanc oriental du bassin de Weber (Indonésie orientale): Comptes Rendus de
238 l'Académie des Sciences - Series IIA - Earth and Planetary Science, v. 325, p. 883–
239 890.
- 240 Hreinsdóttir, S., and Bennett, R.A., 2009, Active aseismic creep on the Alto Tiberina
241 low-angle normal fault, Italy: Geology, v. 37, p. 683–686, doi:10.1130/G30194A.1.
- 242 Lister, G.S., Banga, G., and Feenstra, A., 1984, Metamorphic core complexes of
243 Cordilleran type in the Cyclades, Aegean Sea, Greece: Geology, v. 12, p. 221–225,
244 doi:10.1130/0091-7613(1984)12<221:MCCOCT>2.0.CO;2.
- 245 Lister, G.S., and Davis, G.A., 1989, The origin of metamorphic core complexes and
246 detachment faults formed during Tertiary continental extension in the northern
247 Colorado River region, U.S.A: Journal of Structural Geology, v. 11, p. 65–94,
248 doi:10.1016/0191-8141(89)90036-9.
- 249 Lister, G.S., and Forster, M.A., 2009, Tectonic mode switches and the nature of
250 orogenesis: Lithos, v. 113, p. 274–291, doi:10.1016/j.lithos.2008.10.024.
- 251 Lister, G.S., and Forster, M.A., 2016, White mica $^{40}\text{Ar}/^{39}\text{Ar}$ age spectra and the timing of
252 multiple episodes of high-*P* metamorphic mineral growth in the Cycladic eclogite-

- 253 blueschist belt, Syros, Aegean Sea, Greece: *Journal of Metamorphic Geology*, v. 34,
254 p.401–421, doi:10.1111/jmg.12178.
- 255 Maffione, M., van Hinsbergen, D.J.J., Koornneef, L.M.T., Guilmette, C, Hodges, K.,
256 Borneman, N., Huang, W., Ding, L., and Kapp, P., 2015, Forearc hyperextension
257 dismembered the south Tibetan ophiolites: *Geology*, v. 43, p. 475–478,
258 doi:10.1130/G36472.1.
- 259 McCaffrey, R., 1988, Active tectonics of the eastern Sunda and Banda arcs: *Journal of*
260 *Geophysical Research*, v. 93, p. 15163–15182, doi:10.1029/JB093iB12p15163.
- 261 Milsom, J., 2001, Subduction in eastern Indonesia: how many slabs?: *Tectonophysics*,
262 v. 338, p. 167–178, doi:10.1016/S0040-1951(01)00137-8.
- 263 Pownall, J.M., 2015, UHT metamorphism on Seram, eastern Indonesia: reaction
264 microstructures and P–T evolution of spinel-bearing garnet–sillimanite granulites
265 from the Kobipoto Complex: *Journal of Metamorphic Geology*, v. 33, p. 909–935,
266 doi:10.1111/jmg.12153.
- 267 Pownall, J.M., Hall, R., and Watkinson, I.M., 2013, Extreme extension across Seram and
268 Ambon, eastern Indonesia: evidence for Banda slab rollback: *Solid Earth*, v. 4,
269 p. 277–314, doi:10.5194/se-4-277-2013.
- 270 Pownall, J.M., Hall, R., Armstrong, R.A., and Forster, M.A., 2014, Earth’s youngest
271 known ultrahigh-temperature granulites discovered on Seram, eastern Indonesia:
272 *Geology*, v. 42, p. 279–282, doi:10.1130/G35230.1.
- 273 Royden, L.H., 1993, Evolution of retreating subduction boundaries formed during
274 continental collision: *Tectonics*, v. 12, p. 629–638, doi:10.1029/92TC02641.

- 275 Royden, L.H., and Husson, L., 2009, Subduction with variations in slab buoyancy:
276 Models and application to the Banda and Apennine Systems, *in* Lallemand, S., and
277 Funiciello, F., eds., *Subduction Zone Geodynamics*: Springer-Verlag, Berlin, p. 35–
278 45, doi:10.1007/978-3-540-87974-9_2.
- 279 Schellart, W.P., and Lister, G.S., 2004, Tectonic models for the formation of arc-shaped
280 convergent zones and backarc basins, *in* Sussman, A.J., and Weil, A.B., eds.,
281 *Orogenic Curvature: Integrating Paleomagnetic and Structural Analyses*: Geological
282 Society of America Special Paper 383, p. 237–258, doi:10.1130/0-8137-2383-
283 3(2004)383[237:TMFTFO]2.0.CO;2.
- 284 Spakman, W., and Hall, R., 2010, Surface deformation and slab–mantle interaction
285 during Banda arc subduction rollback: *Nature Geoscience*, v. 3, p. 562–566,
286 doi:10.1038/ngeo917.
- 287 Spencer, J.E., 1984, The role of tectonic denudation in the warping and uplift of low-
288 angle normal faults: *Geology*, v. 12, p. 95–98, doi:10.1130/0091-
289 7613(1984)12<95:ROTDIW>2.0.CO;2.
- 290 Spencer, J.E., 2010, Structural analysis of three extensional detachment faults with data
291 from the 2000 Space-Shuttle Radar Topography Mission: *GSA Today*, v. 20, p. 4–
292 10, doi:10.1130/GSATG59A.1.
- 293 Tate, G.W., McQuarrie, N., van Hinsbergen, D.J.J., Bakker, R.R., Harris, R., and Jiang,
294 H., 2015, Australia going down under: Quantifying continental subduction during
295 arc-continent accretion in Timor-Leste: *Geosphere*, v. 11, p. 1860–1883,
296 doi:10.1130/GES01144.1.

297 Wernicke, B., 1995, Low-angle normal faults and seismicity: A review: Journal of
298 Geophysical Research, v. 100, p. 20159–20174, doi:10.1029/95JB01911.
299 Wright, L.A., Otton, J.K., and Troxel, B.W., 1974, Turtleback surfaces of Death Valley
300 viewed as phenomena of extensional tectonics: Geology, v. 2, p. 53–54,
301 doi:10.1130/0091-7613(1974)2<53:TSODVV>2.0.CO;2.

302

303 FIGURE CAPTIONS

304

305 Figure 1. Bathymetric map of the Weber Deep and Aru Trough, showing the location of
306 the Banda Detachment and its relationship to the Kawa Shear Zone on Seram. Purple
307 areas mark approximate exposures of exhumed upper-mantle/lower-crustal (Kobipoto
308 Complex) rocks. MULTIBEAM data (15 m resolution) courtesy of TGS and GeoData
309 Ventures. See Fig. 2 for location map; Figs. 3, DR1, and DR2 for enlargements of yellow
310 boxes; Fig. 4 for photos of the Banda Detachment; Fig. 5 for cross section X–X'; and Fig.
311 DR4 for a 3D visualization.

312

313 Figure 2. Map of eastern Indonesia showing the location of the Banda Arc, and the extent
314 of MULTIBEAM bathymetry data used in Fig. 1.

315

316 Figure 3. A, B: Enlargements of bathymetric map (marked by yellow boxes in Fig. 1)
317 showing grooved normal fault surfaces comprising the fluted Banda Detachment
318 footwall, analogous to the ‘turtlebacks’ of Death Valley (Wright et al., 1974). Note the
319 consistent 130–310° orientations, which are parallel to the inferred slip direction and also

320 to the trend of the Kawa Shear Zone on Seram. Further examples are shown in Figs. DR1
321 and DR2.

322

323 Figure 4. The Banda Detachment, exposed on land in A: Eastern Seram (130.03°E,
324 3.46°S), and B: the island of Fadol (131.94°E, 5.67°S). Both fault planes dip towards the
325 Banda Sea at 12° – identical to the dip inferred from Fig. 1.

326

327 Figure 5. A: Cross section X–X' (located in Figure 1; no vertical exaggeration) through
328 the eastern Banda Arc, cut parallel to the grooves on fault surfaces and the proposed
329 direction of rollback (130°SE). The geometry of the Proto-Banda Sea Slab is inferred
330 from earthquake hypocenter locations catalogued by the International Seismological
331 Centre Online Bulletin (isc.ac.uk). KSZ—Kawa Shear Zone. B: Enlargement of the
332 Banda Detachment (2 × vertical exaggeration) showing schematically the configuration
333 of over-riding continental allochthons (dark red).

334

335 ¹GSA Data Repository item xxxxxx, additional examples of grooved normal fault scarps
336 flooring the Weber Deep (Fig. DR1 and DR2) a low-angle extensional shear zone on
337 Kasiui (Fig. DR3), and a 3D visualization of the Weber Deep (Fig. DR4), is available
338 online at www.geosociety.org/pubs/ft2015.htm, or on request from
339 editing@geosociety.org.

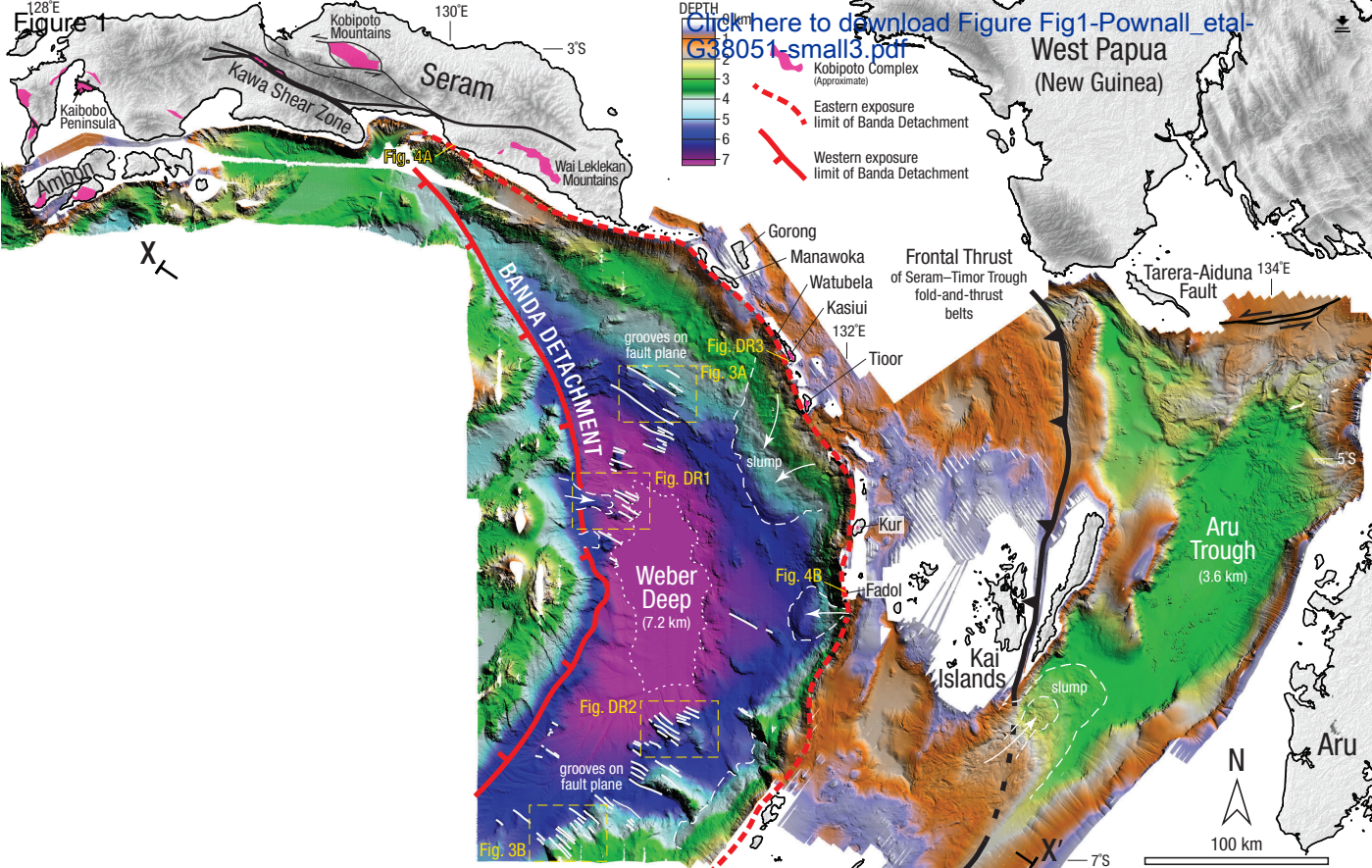
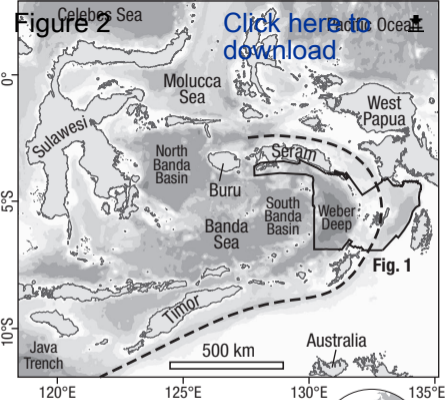


Figure 2

[Click here to download](#)



 Extent of 15 m MULTIBEAM bathymetry dataset

 BANDA ARC
Seram Trough & Timor Trough

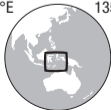
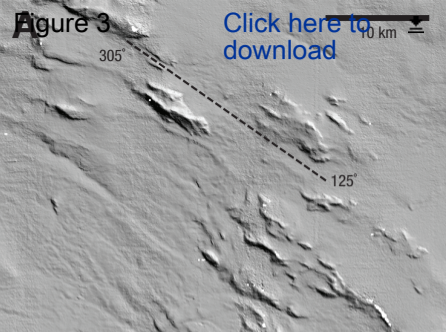


Figure 3

[Click here to download](#)



B

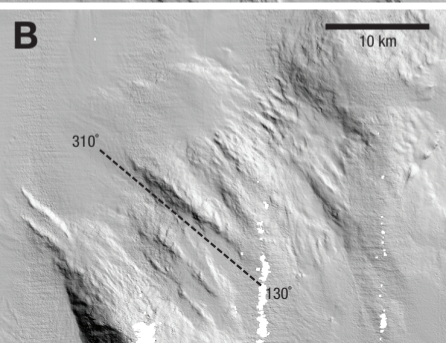
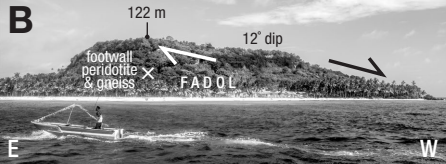


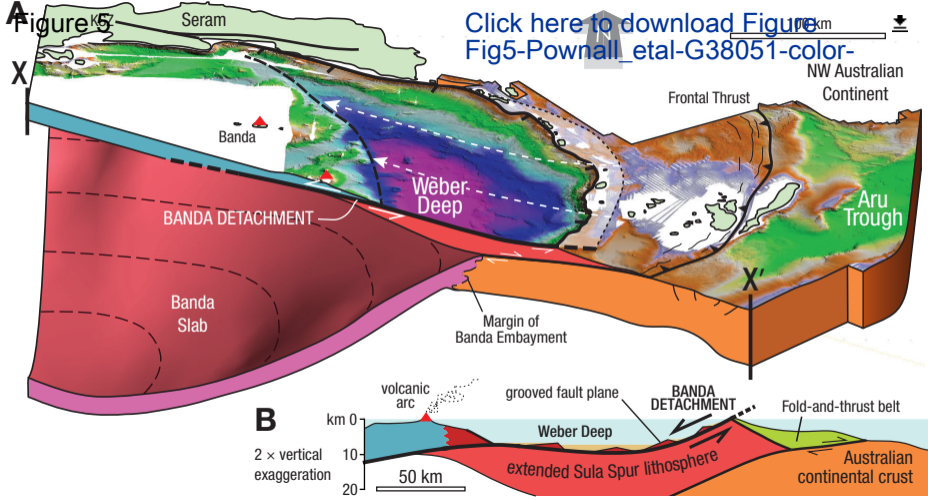
Figure 4

[Click here to download](#)



B





Pownall et al.
Rolling open Earth's deepest forearc basin

DATA REPOSITORY ITEMS

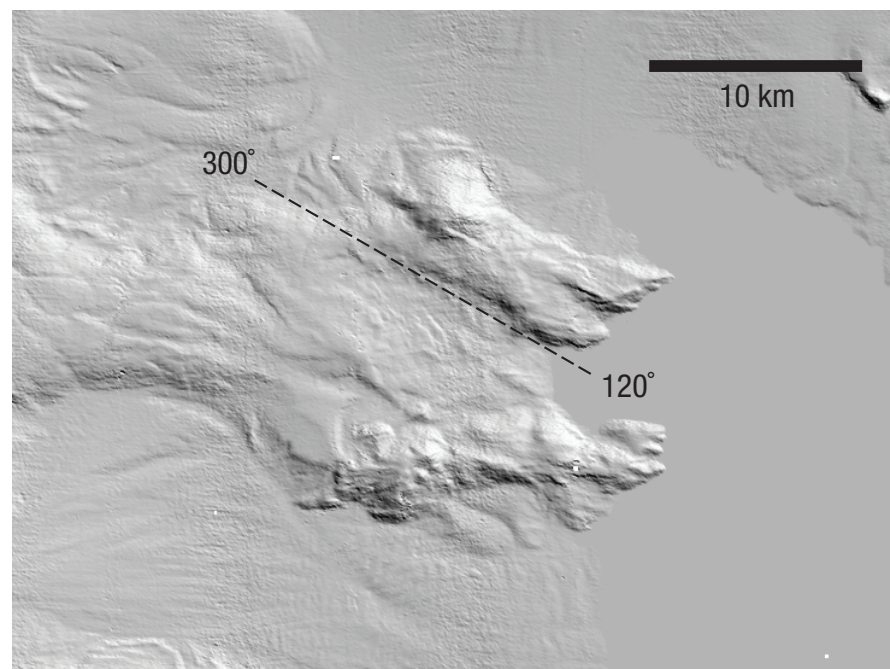


Figure DR1. Enlargement of yellow box 'DR1' in Figure 1. Normal fault scarp grooves have 300–120° orientation.

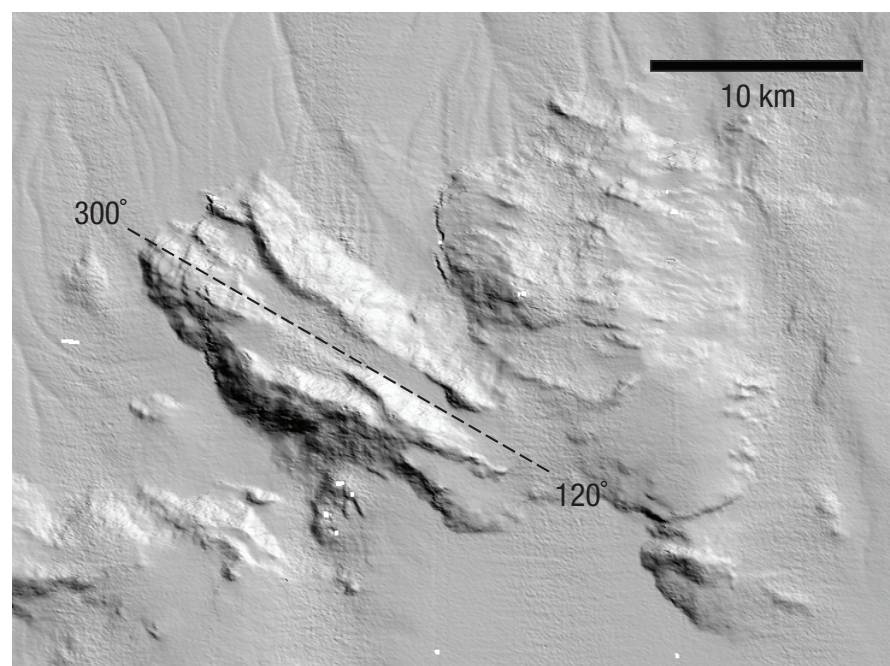


Figure DR2. Enlargement of yellow box 'DR2' in Figure 1. Normal fault scarp grooves have 300–120° orientation.

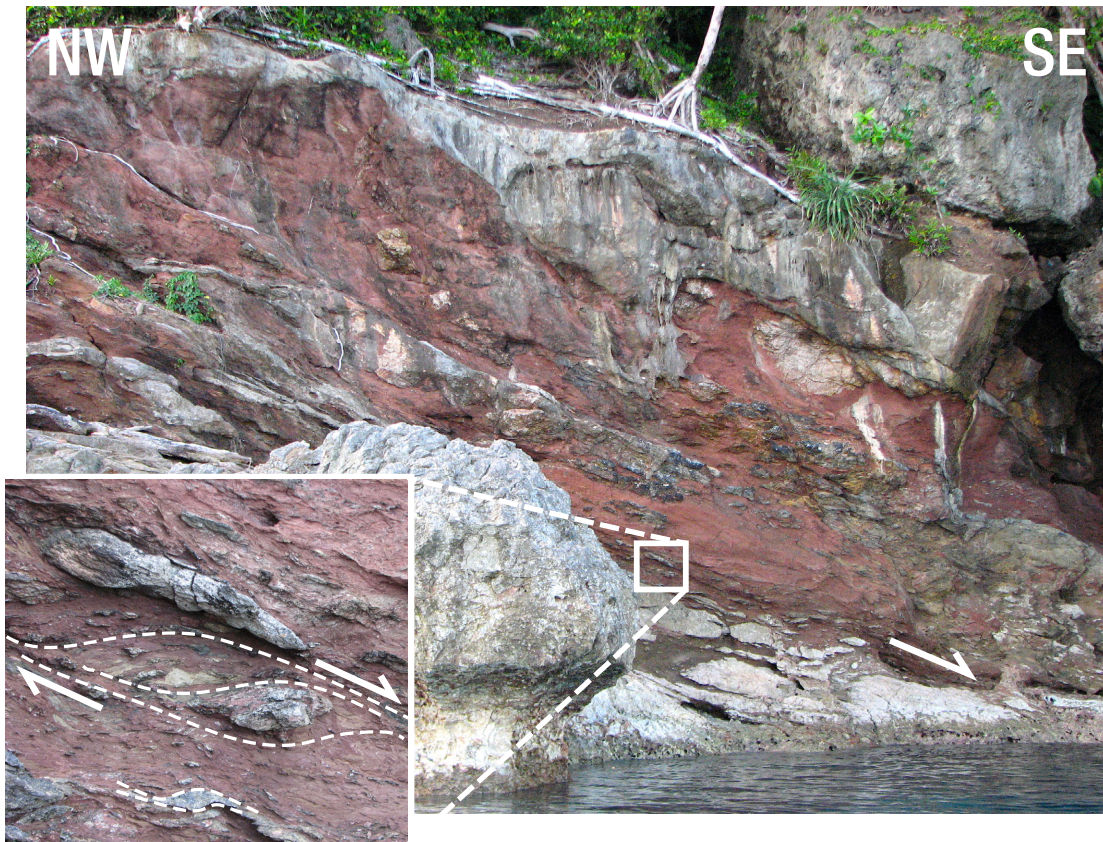


Figure DR3. Low-angle extensional normal shear zone, south Kasiui (131.6776°E , 4.5394°S), dipping 20° to 345°NNW . Enlarged box is 0.6 m wide.

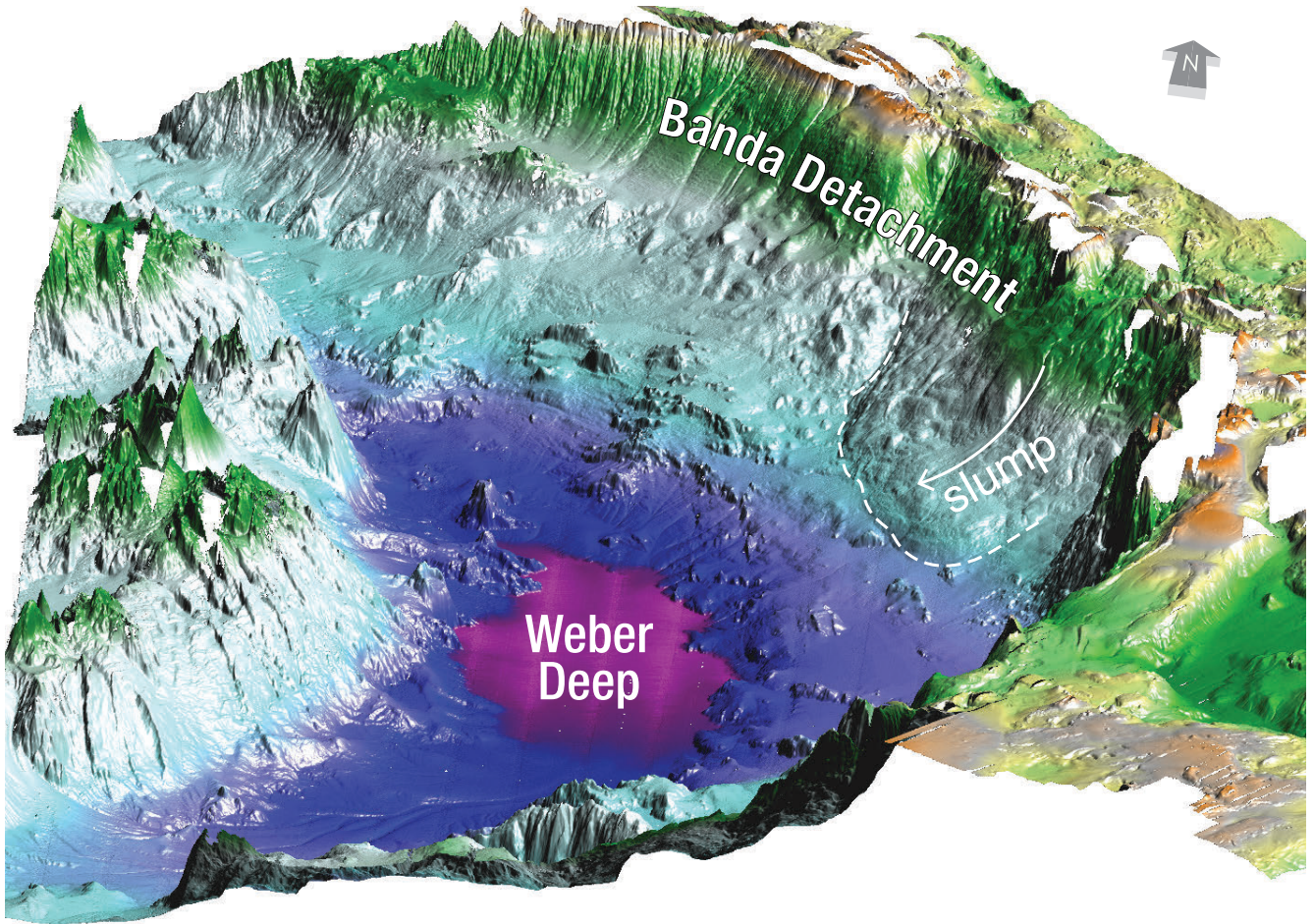


Figure DR4. 3D visualization of the Weber Deep, produced from the MULTIBEAM data used also in Fig. 1.